

Chapter 12

RAFT FOUNDATIONS

12.1 Strip Foundations on a Semi-Infinite Mass

12.1.1 BEHAVIOUR IN TRANSVERSE DIRECTION

(a) Smooth Strip Subjected to Uniform Pressure

Borowicka (1939) has obtained solutions for the distribution of contact pressure p beneath a strip subjected to uniform pressure q . These solutions are shown in Fig.12.1. The relative stiffness K is defined as

$$K = \frac{1}{6} \frac{(1-v_s^2)}{(1-v_p^2)} \frac{E_p}{E_s} \left(\frac{t}{b} \right)^3 \quad \dots (12.1)$$

where E_p, v_p = elastic moduli of strip

t = strip thickness

b = half width of strip

E_s, v_s = elastic moduli of mass.

(b) Smooth Strip Subjected to Central Line Load

Borowicka (1939) has obtained the solutions shown in Fig.12.2 for the contact pressure distribution p beneath the strip. $p_{av}=P/2b$ where P is the line load per unit length, and K is defined in Equation (12.1).

(c) Rough Strip Subjected to Uniform Pressure

Lee (1963) obtained solutions for the contact normal and shear stresses and the bending moments and the shear forces within the strip. For v_s of the soil =0, the contact normal stresses are shown in Fig.12.3, contact shear stresses in Fig.12.4, distributions of bending moment in Fig.12.5, and distributions of shearing force in Fig.12.6. In these figures the relative stiffness K is defined as

$$K = \frac{2E_p I_p}{(1-v_p^2) E_s b^3} \quad \dots (12.1)$$

where E_p, v_p = the elastic moduli of strip

$t^3/12 = I_p$ = moment of inertia of strip

E_s = Young's modulus of soil

b = half-width of strip.

The variation of maximum shearing force, maximum bending moment and maximum differential settlement with K is shown in Figs.12.7, 12.8 and 12.9 respectively.

It should be noted that if $v_s=0.5$, the solutions for a rough strip are identical with those for a smooth strip.

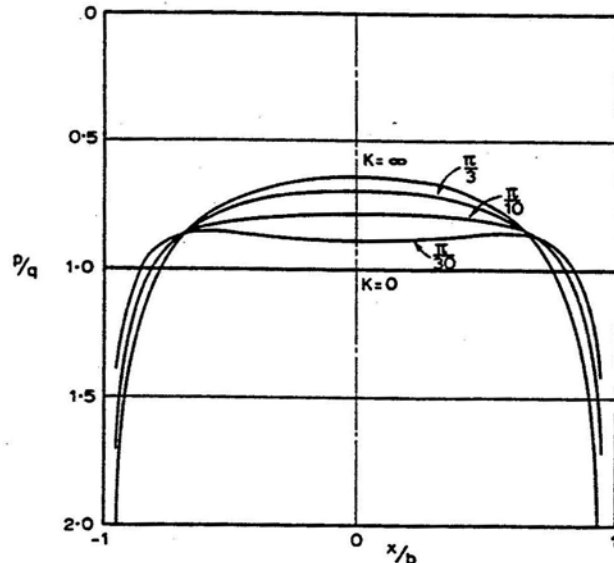


FIG.12.1 Contact pressure distribution beneath uniformly loaded smooth strip (Borowicka, 1939).

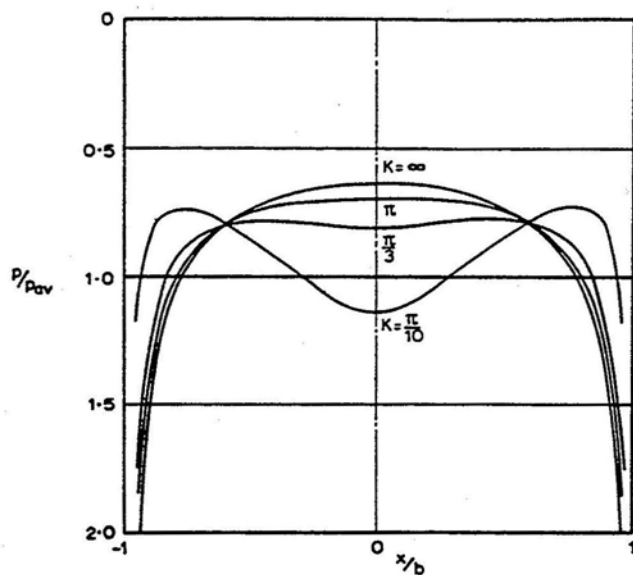


FIG.12.2 Contact pressure distribution beneath smooth strip with line load (Borowicka, 1939).

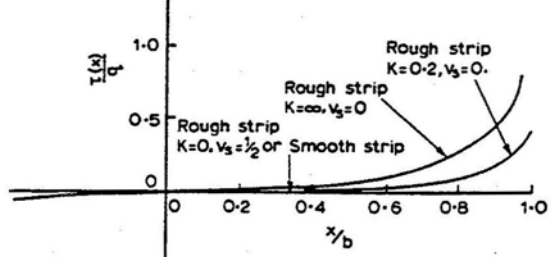


FIG.12.4 Contact shear stress beneath uniformly loaded rough strip (Lee, 1963).

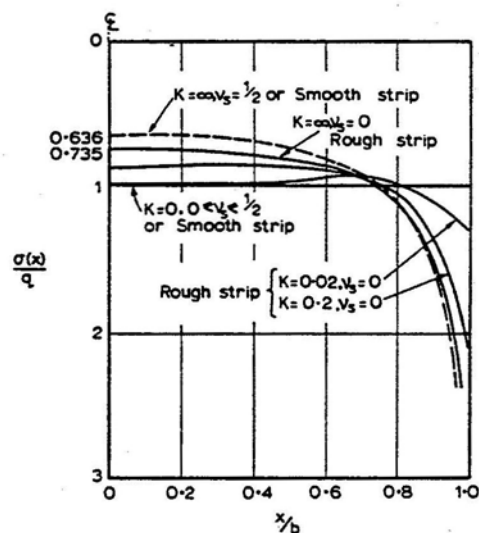


FIG.12.3 Vertical contact stress beneath uniformly loaded rough strip (Lee, 1963).

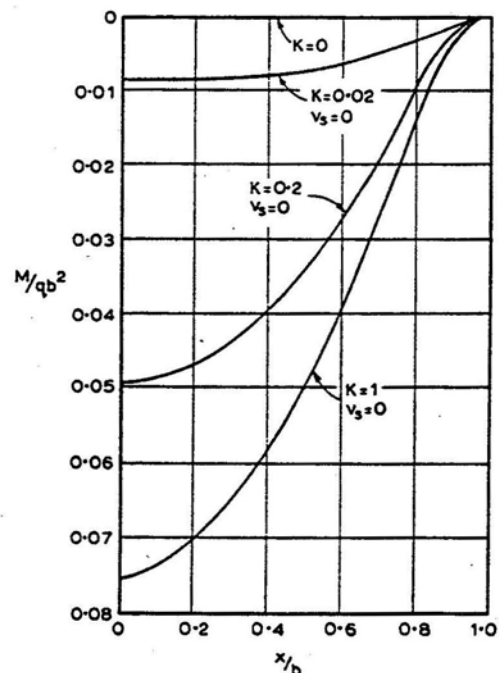


FIG.12.5 Bending moments in uniformly loaded rough strip (Lee, 1963).

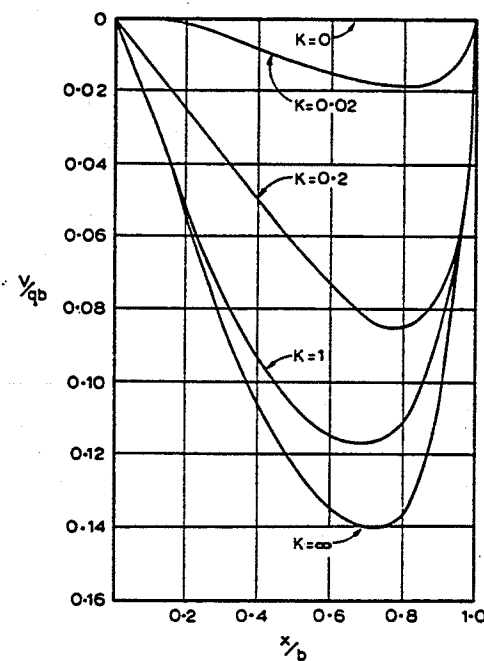


FIG.12.6 Shear force in uniformly loaded rough strip.
 $v_s = 0$. (Lee, 1963).

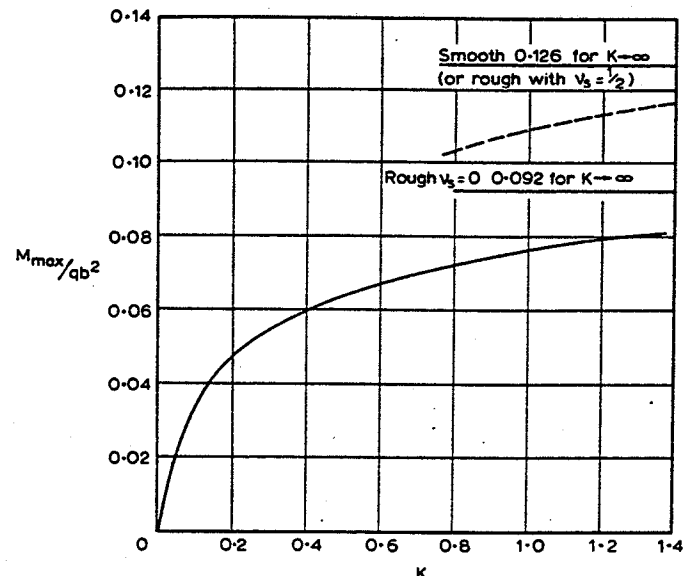


FIG.12.8 Maximum bending moment in uniformly loaded strip (Lee, 1963).

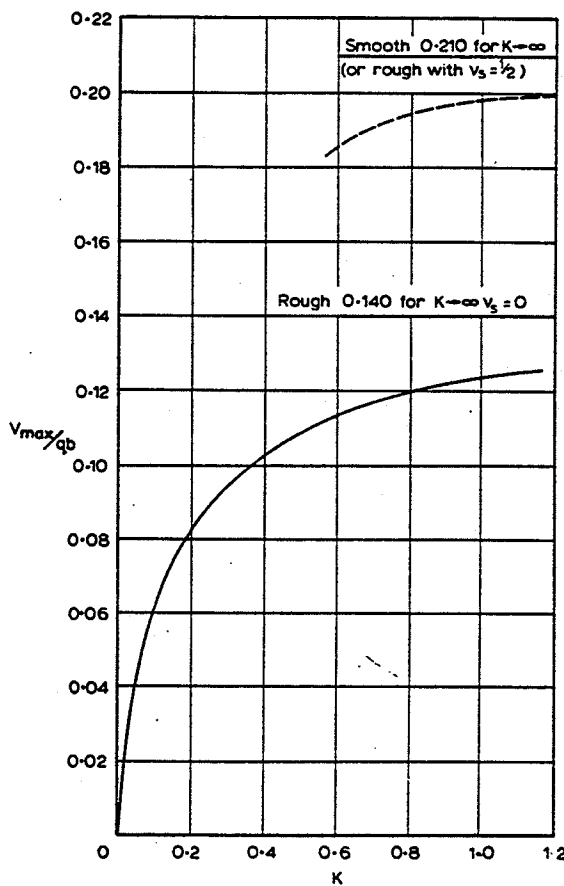


FIG.12.7 Maximum shear force in uniformly loaded strip (Lee, 1963).

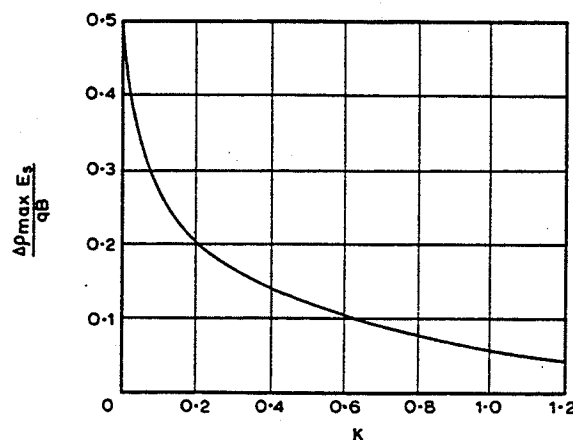


FIG.12.9 Maximum differential deflection in uniformly loaded rough strip. $v_s = 0$. (Lee, 1963).

12.1.2 BEHAVIOUR IN LONGITUDINAL DIRECTION

- (a) Vertical and Moment Loading on Infinite Strip (Fig.12.10)

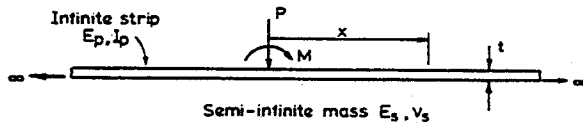


FIG.12.10

Biot (1937) obtained a solution for the maximum bending moment beneath an infinitely long smooth strip loaded by a concentrated load. Vesic (1961) extended Biot's work and obtained the following solutions for deflection, rotation, moment, shear and pressure, for both vertical loading and for moment loading.

Concentrated Loading:

$$\text{Deflection } \rho = \frac{Pc^3}{\pi E_p I_p} J_0(x) \quad \dots (12.3)$$

$$\text{Slope } \theta = -\frac{Pc^2}{\pi E_p I_p} J_1(x) \quad \dots (12.4)$$

$$\text{Moment } M = \frac{Pc}{\pi} J_2(x) \quad \dots (12.5)$$

$$\text{Shear } V = -\frac{P}{\pi} J_3(x) \quad \dots (12.6)$$

$$\text{Pressure } p = \frac{P}{c\pi} J_4(x) \quad \dots (12.7)$$

Moment Loading:

$$\text{Deflection } \rho = \frac{Mc^2}{\pi E_p I_p} J_1(x) \quad \dots (12.8)$$

$$\text{Slope } \theta = \frac{Mc}{\pi E_p I_p} J_2(x) \quad \dots (12.9)$$

$$\text{Moment } M = \frac{M}{\pi} J_3(x) \quad \dots (12.10)$$

$$\text{Shear } V = -\frac{M}{c\pi} J_4(x) \quad \dots (12.11)$$

$$\text{Pressure } p = \frac{M}{c^2\pi} J_5(x) \quad \dots (12.12)$$

In the above equations,

$$c = [C(1-v_s^2) \frac{E_p I_p}{E_s}]^{1/3} \quad \dots (12.13)$$

$C = 1.00$ assuming constant reaction pressure across width of strip

or $1.00 < C < 1.13$ assuming constant deflection across width of strip

$E_p I_p$ = stiffness of beam ($I_p = t^3/12$)

E_s, v_s = elastic moduli of underlying mass

b = half-width of strip.

$P, M & V$ are per unit width.

The functions $J_0(x)$ etc. are given approximately as follows:

$$J_0(x) = 1.370 \left(\frac{b}{c}\right)^{0.587} e^{-\lambda x} (\cos \lambda x \sin \lambda x) \quad \dots (12.14a)$$

$$J_1(x) = 0.244 \left(\frac{b}{c}\right)^{0.333} e^{-\lambda x} \sin \lambda x \quad \dots (12.14b)$$

$$J_2(x) = 0.332 \left(\frac{b}{c}\right)^{0.169} e^{-\lambda x} (\cos \lambda x - \sin \lambda x) \quad \dots (12.14c)$$

$$J_3(x) = \frac{\pi}{2} e^{-\lambda x} \cos \lambda x \quad \dots (12.14d)$$

$$J_4(x) = 1.285 \left(\frac{b}{c}\right)^{-0.155} e^{-\lambda x} (\cos \lambda x + \sin \lambda x) \quad \dots (12.14e)$$

$$J_5(x) = 0.259 \left(\frac{b}{c}\right)^{-0.360} e^{-\lambda x} \sin \lambda x \quad \dots (12.14f)$$

$$\text{where } \lambda = \frac{0.689}{b} \left(\frac{b}{c}\right)^{0.813}$$

(b) Concentrated Loading on Finite Strip

For strips of finite length, Brown (1969c) gives solutions for the distribution of deflection and bending moment due to a single concentrated load at various positions on the strip. These solutions, for various values of relative stiffness K , are shown in Figs.12.11 to 12.14 for bending moment, and in Figs.12.15 to 12.18 for deflection. In this case, K is defined as

$$K = \frac{E_p I_p (1-v_s^2)}{\pi E_s a^4} \quad \dots (12.15)$$

where E_p = modulus of strip

I_p = moment of inertia of strip section = $bt^3/6$

E_s, v_s = moduli of foundation

a = $\frac{1}{2}$ length of strip

b = $\frac{1}{2}$ width of strip.

The average contact pressure $q=1/4ba$ (for unit applied load). Brown has found that the ratio a/b has a relatively small influence on the moments.

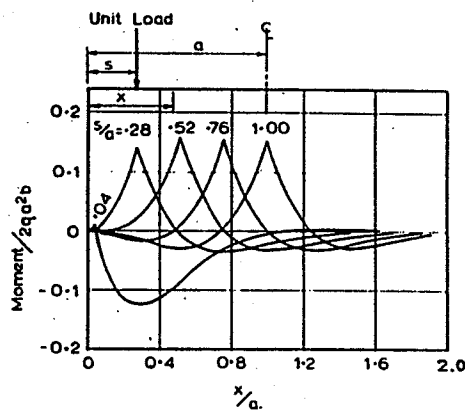


FIG.12.11 Moment in strip.
 $a/b=25$, $K=4.1 \times 10^{-4}$.
(Brown, 1969c).

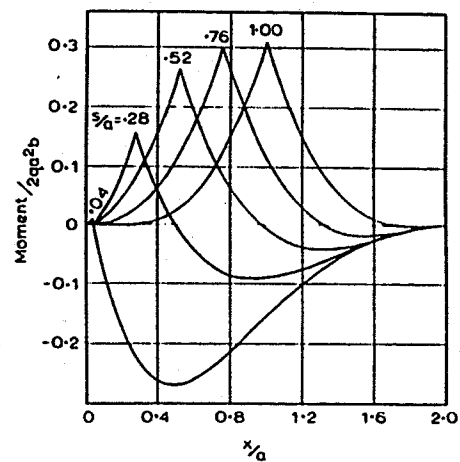


FIG.12.12 Moment in strip.
 $a/b=25$, $K=4.1 \times 10^{-4}$.
(Brown, 1969c).

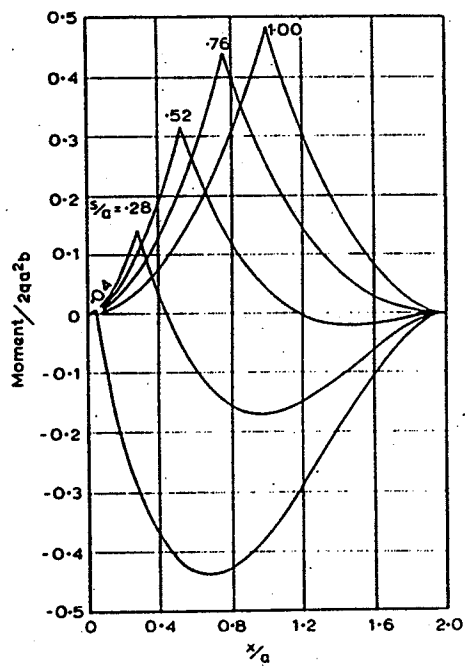


FIG.12.13 Moment in strip.
 $a/b=25$, $K=4.1 \times 10^{-2}$.
(Brown, 1969c).

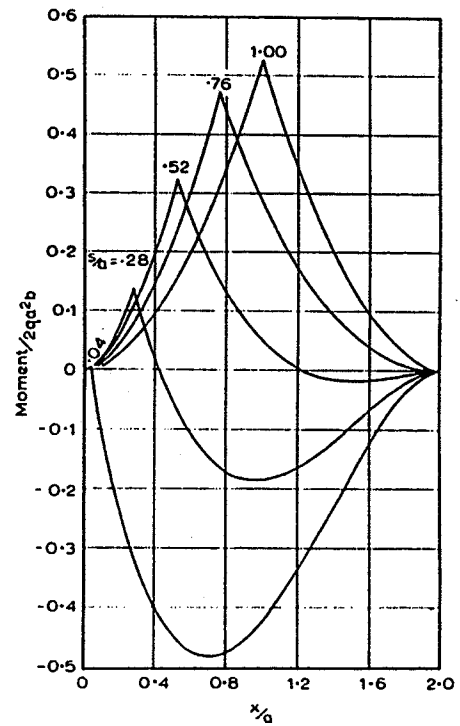


FIG.12.14 Moment in strip.
 $a/b=25$, $K=4.1 \times 10^{-1}$.
(Brown, 1969c).

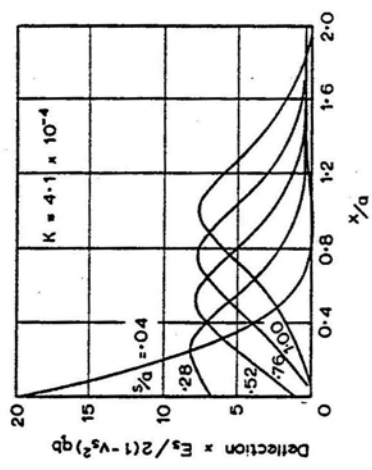


FIG.12.15 Deflection along strip.
 $a/b=25$, $K=4.1 \times 10^{-4}$.
(Brown, 1969c).

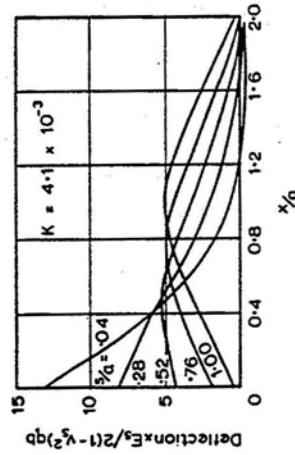


FIG.12.16 Deflection along strip.
 $a/b=25$, $K=4.1 \times 10^{-3}$.
(Brown, 1969c).

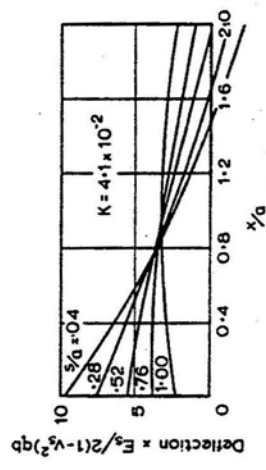


FIG.12.17 Deflection along strip.
 $a/b=25$, $K=4.1 \times 10^{-2}$.
(Brown, 1969c).

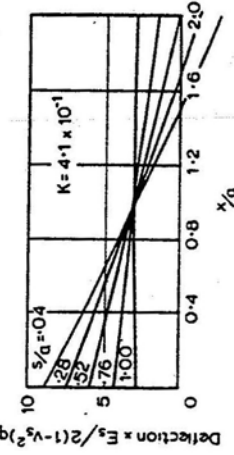


FIG.12.18 Deflection along strip
 $a/b=25$, $K=4.1 \times 10^{-1}$.
(Brown, 1969c).

(c) Uniform Loading on Smooth Finite Strip

Brown (1969c) has obtained solutions for the maximum moment, maximum differential deflection and central deflection of the strip. These solutions are shown in Figs. 12.19 to 12.21 for 3 values of a/b . In all cases, ν of the strip = 0.3. The uniform applied pressure = q /unit area.

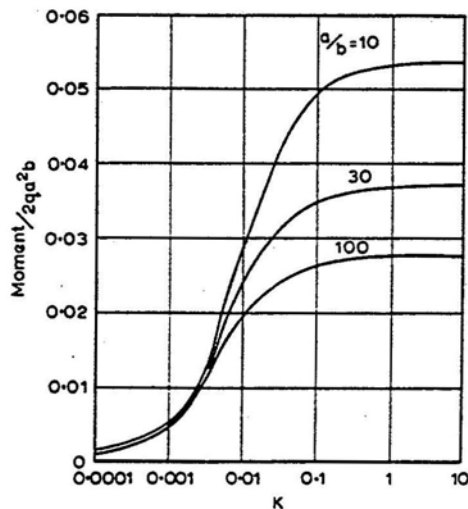


FIG.12.19 Maximum moment in uniformly loaded strip (Brown, 1969c).

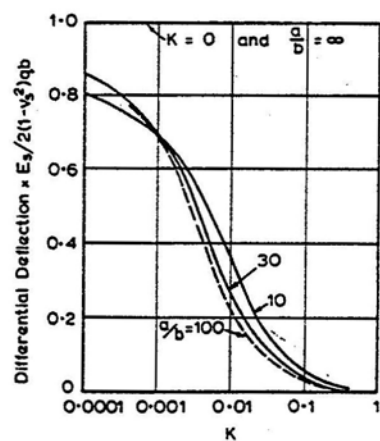


FIG.12.20 Differential deflection in uniformly loaded strip (Brown, 1969c).

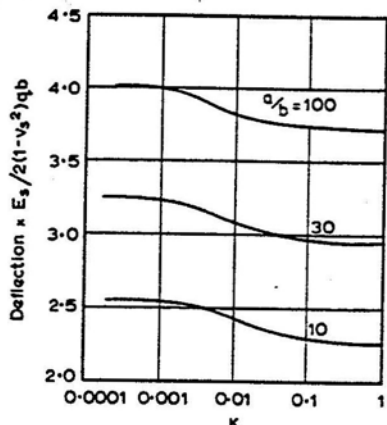


FIG.12.21 Central deflection of uniformly loaded strip (Brown, 1969c).

12.2 Circular Rafts

12.2.1 CIRCULAR RAFT ON SEMI-INFINITE MASS

(a) Uniform Loading

This problem was considered by Borowicka (1939) and more recently by Brown (1969b) (refer also to Section 7.2).

Influence factors obtained by Brown for the central vertical displacement of the raft at the surface are given in Fig.12.22 for Poisson's ratio ν_p of the raft of 0.3. The relative flexibility of the raft is expressed in terms of a factor K where

$$K = \frac{E_p}{E_s} (1-\nu_p^2) \left(\frac{t}{a}\right)^3 \quad \dots (12.16)$$

where E_p = Young's modulus of raft
 t = raft thickness
 a = raft radius
 E_s, ν_s = elastic moduli of soil

Distributions of contact pressure are shown in Fig.12.23 for various values of K . Bending moment distributions are shown in Fig.12.24 while the variation of maximum moment with K is shown in Fig.12.25. Tabulated values of radial and tangential moment per unit width are given in Table 12.1. The variation of maximum differential deflection is shown in Fig.12.26. In all cases, q =applied uniform pressure.

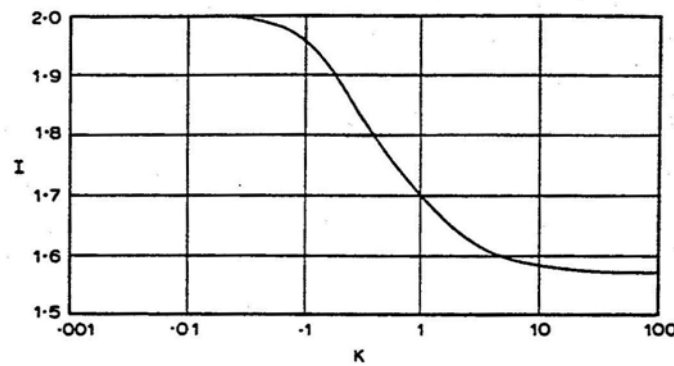


FIG.12.22 Central vertical displacement factor for circular raft (Brown, 1969b)

$$\rho = \frac{qa(1-\nu_s^2)I}{E_s}$$

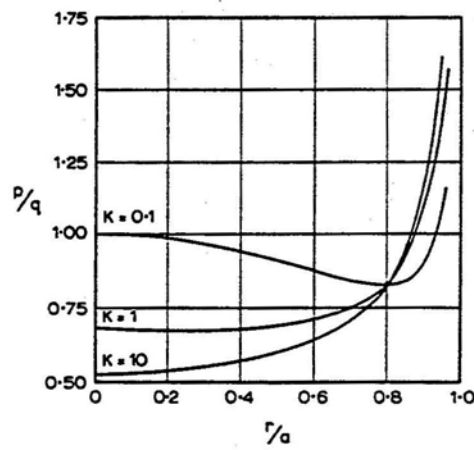


FIG.12.23 Contact pressure beneath circular raft.
 $\nu_p=0.3$. (Brown, 1969b).

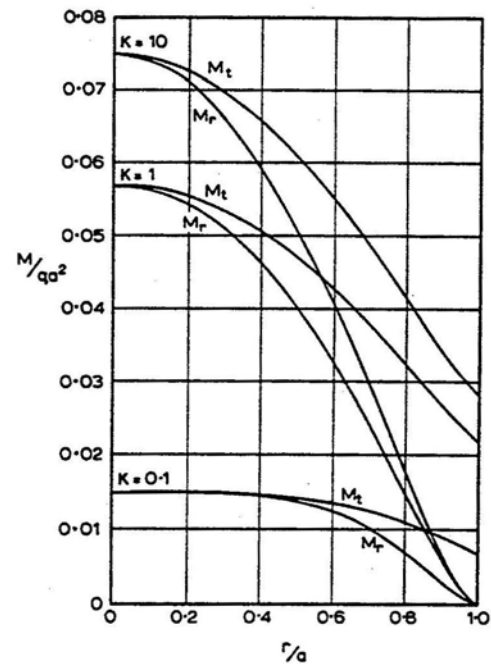


FIG.12.24 Bending moment distributions in circular raft. $\nu_p=0.3$. (Brown, 1969b).

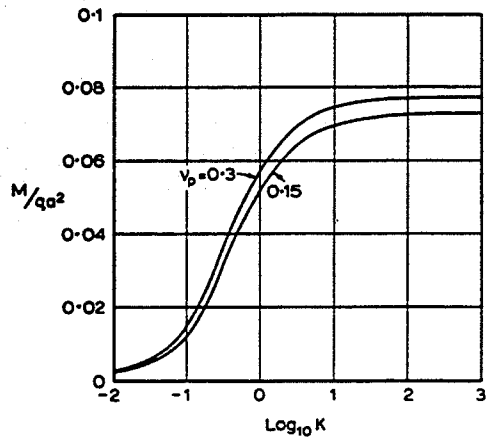


FIG.12.25 Maximum moment in circular raft (Brown, 1969b).

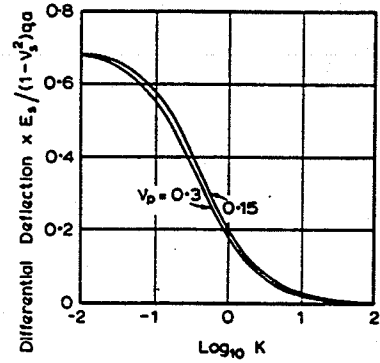


FIG.12.26 Differential deflection in circular raft (Brown, 1969b).

TABLE 12.1
BENDING MOMENTS IN CIRCULAR RAFT ON SEMI-INFINITE MASS
Values of $\frac{M}{q\alpha^2}$ for $v_p=0.3$
(Brown, 1969b)

K	10		1		0.1		0.01	
	$\frac{r}{a}$	M_r	M_t	M_r	M_t	M_r	M_t	M_r
0	0.0747	0.0747	0.0567	0.0567	0.0146	0.0146	0.0012	0.0012
0.1	0.0737	0.0741	0.0561	0.0564	0.0146	0.0146	0.0012	0.0012
0.2	0.0708	0.0724	0.0541	0.0552	0.0146	0.0146	0.0013	0.0012
0.3	0.0659	0.0696	0.0508	0.0533	0.0145	0.0146	0.0014	0.0013
0.4	0.0593	0.0658	0.0461	0.0506	0.0142	0.0144	0.0016	0.0014
0.5	0.0509	0.0609	0.0401	0.0472	0.0136	0.0142	0.0018	0.0015
0.6	0.0411	0.0551	0.0329	0.0430	0.0125	0.0136	0.0021	0.0017
0.7	0.0301	0.0486	0.0246	0.0381	0.0106	0.0127	0.0024	0.0019
0.8	0.0184	0.0415	0.0154	0.0327	0.0076	0.0114	0.0024	0.0020
0.9	0.0072	0.0343	0.0063	0.0271	0.0037	0.0095	0.0017	0.0018
1.0	0	0.0283	0	0.0222	0	0.0074	0	0.0012

(b) Concentrated Loading

Borowicka (1939) has obtained solutions for the contact pressure p beneath the raft. These are shown in Fig.12.27. $p_{av} = P/\pi a^2$, and the stiffness factor is defined as

$$K = \frac{1}{6} \frac{(1-\nu_p^2)}{p} \frac{E_p}{E_s} \left(\frac{t}{a} \right)^3 \quad \dots (12.17)$$

where t = raft thickness
 a = raft radius.

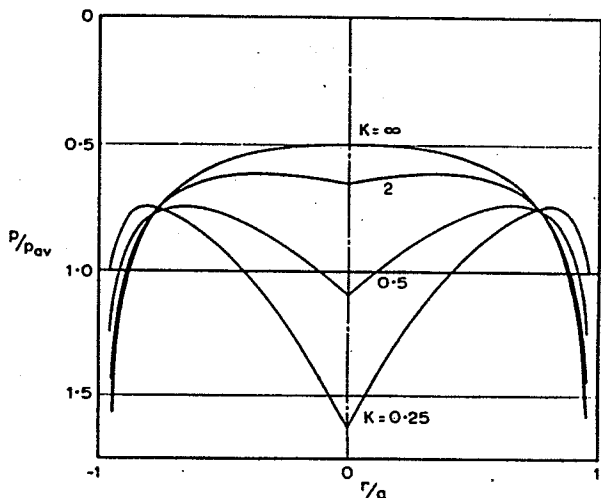


FIG.12.27 Contact pressure distribution beneath circular raft with central point loading (Borowicka, 1939).

λ, G = Lame's parameters of the mass.

r = radial distance from point load

ρ_z = vertical displacement.

For a uniformly distributed load, the displacement beneath the centre is almost the same as that due to a concentrated loading provided that the radius of the loading is of the same order as the thickness t .

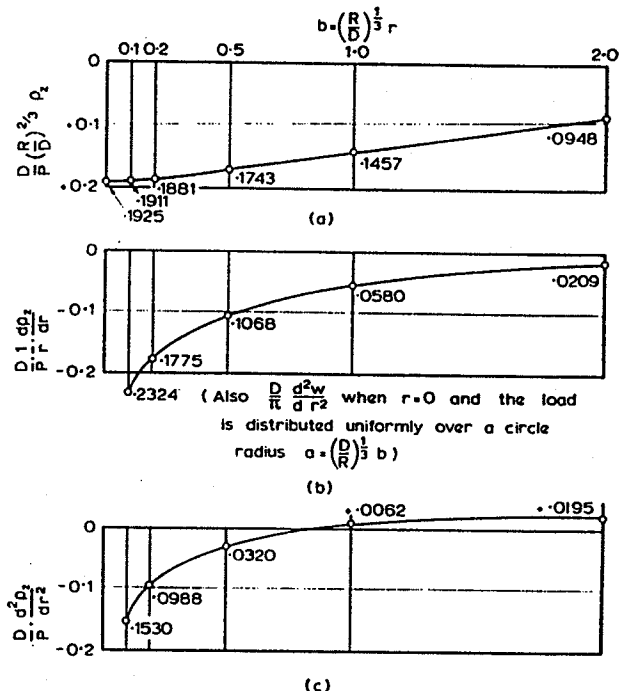


FIG.12.28 Displacement, slope and curvature of uniform thin raft with point loading (Hogg, 1938).

For a raft of infinite extent on a semi-infinite elastic mass, and loaded by a point load P , Hogg (1938) has obtained solutions for the displacement and curvature of the raft. These are shown in Fig.12.28, where

$$D = \text{flexural rigidity of raft} = \frac{E_p t^3}{12(1-\nu_p^2)}$$

t = raft thickness

$$R = \frac{2G(\lambda+2G)}{\lambda+3G} \quad \text{for perfectly rough plate}$$

$$\text{or } \frac{2G(\lambda+G)}{\lambda+2G} \quad \text{for perfectly smooth plate}$$

12.2.2 RIGID CIRCULAR RAFT ON A FINITE LAYER

This problem has been considered by Egorov and Serebryanyi (1963) and Poulos (1968a).

Influence factors for the displacement of the raft have been given in Fig. 7.19.

Distributions of contact pressure beneath the raft are given in Figs. 7.15 and 7.16.

For a raft having $v_p=0.25$, the distributions of radial and tangential bending moments are shown in Figs. 12.29 and 12.30 for a uniformly distributed load over the raft and in Figs. 12.31 and 12.32 for a load concentrated within $r=0.1a$ near the centre of the raft. In these figures, v_s of the layer = 0.4. The influence of varying v_s on the central moment for a uniformly distributed loading is shown in Fig. 12.33 for various values of layer depth h to raft radius a .

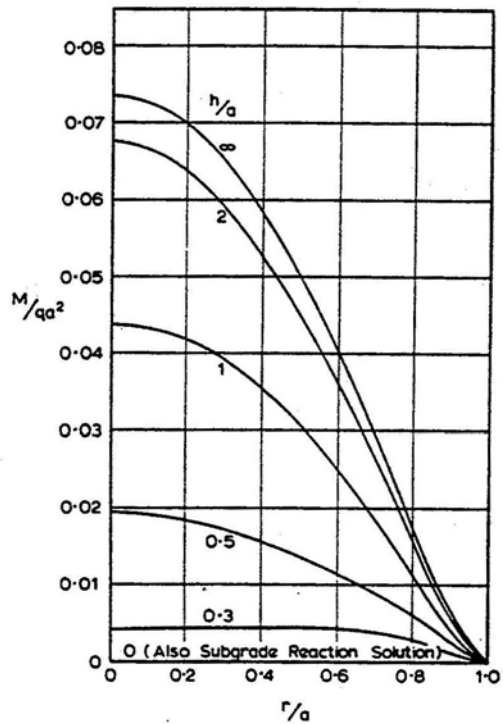


FIG.12.29 Radial bending moment distribution in uniformly loaded rigid circular raft.
 $v_s=0.4$, $v_p=0.25$.

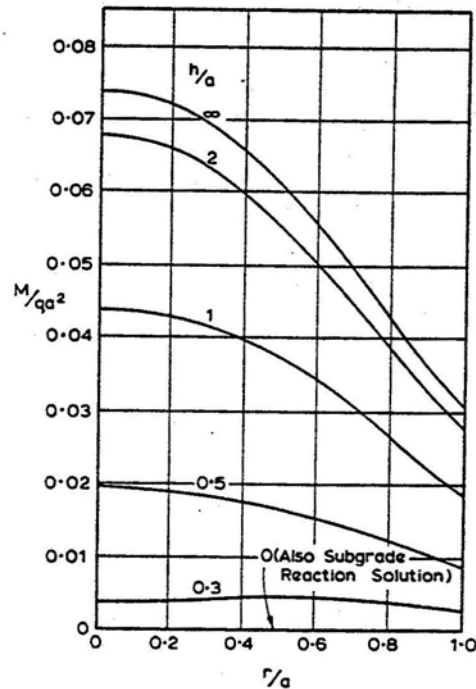


FIG.12.30 Tangential bending moment distribution in uniformly loaded rigid circular raft.
 $v_s=0.4$, $v_p=0.25$.

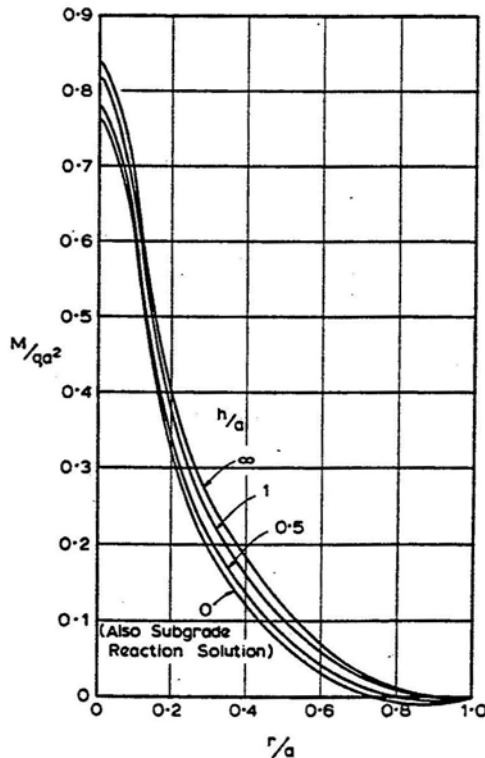


FIG.12.31 Radial bending moment distribution for concentrated load within $r=0.1a$.
 $v_s=0.4$, $v_p=0.25$.

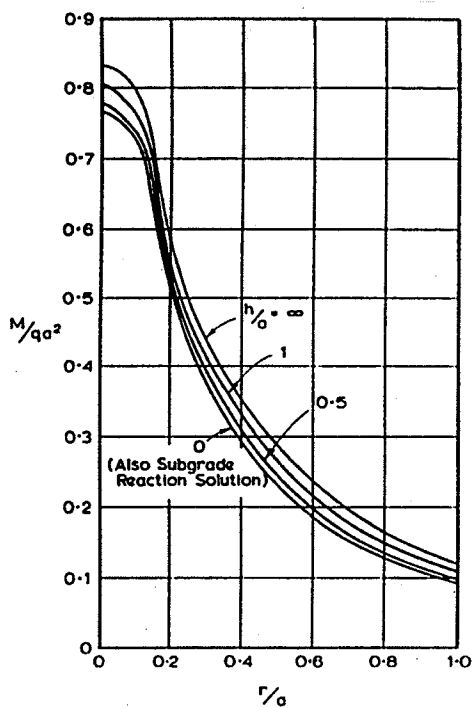


FIG.12.32 Tangential bending moment distribution for concentrated loading within $r=0.1a$.

$$v_s = 0.4, \quad v_p = 0.25.$$

12.2.3 CIRCULAR RAFT OF ANY FLEXIBILITY ON A FINITE LAYER (Uniform Loading)

This problem has been considered by Brown (1969a).

The relative flexibility of the raft is defined by a factor K where

$$K = \frac{E_p(1-v_s^2)}{E_s} \left(\frac{t}{a}\right)^3 \quad \dots (12.18)$$

where t = raft thickness

a = raft radius.

For $h/a=1$, distributions of contact pressure beneath the raft are shown in Fig.12.34 for three values of K .

The variation of central vertical surface displacement with a/h is shown in Fig.12.35 for two values of K .

The variation of differential vertical displacement between centre and edge with K is shown in Fig.12.36.

For uniformly distributed loading over the raft, bending moment distributions are shown in Fig.12.37 for $h/a=1$. The influence of h/a on the bending moment distributions is shown in Fig.12.38 for $K=0.1$.

The variation of maximum (central) moment with K for various h/a values is shown in Fig.12.39.

12.3 Rectangular Rafts

12.3.1 RIGID RAFT ON SEMI-INFINITE MASS

Gorbunov-Possadov and Serebrjanyi (1961) have obtained solutions for the moments, shear force and pressure distribution within a rigid square slab subjected to a central concentrated load. Influence factors are shown in Fig.12.40.

$$\text{Contact pressure } p = \bar{p} \cdot p_{av} \quad \dots (12.19a)$$

$$\text{Shear force } N_x = \bar{N}_x \cdot a \cdot p_{av} \quad \dots (12.19b)$$

$$\text{Bending moment } M_x = \bar{M}_x \cdot a^2 \cdot p_{av} \quad \dots (12.19c)$$

$$\text{Torsional moment } H_x = \bar{H}_x \cdot a^2 \cdot p_{av} \quad \dots (12.19d)$$

where $a = \frac{1}{2}$ width of square

$$p_{av} = \text{average applied pressure} = \frac{P}{4a^2}$$

$P = \text{total load.}$

A rectangular slab ($2a \times 2b$) can be considered as rigid if

$$\frac{\pi a^2 b E_s}{D(1-v_s^2)} < \frac{8}{\left(\frac{b}{a}\right)^{\frac{1}{2}}} \quad (b>a) \quad \dots (12.20)$$

where D is defined on p.258

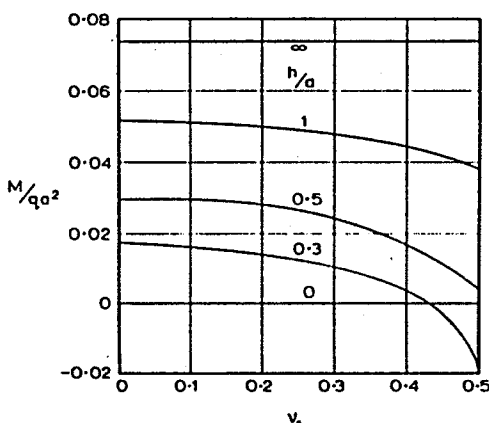


FIG.12.33 Influence of v_s on central bending moment.
Uniform loading.

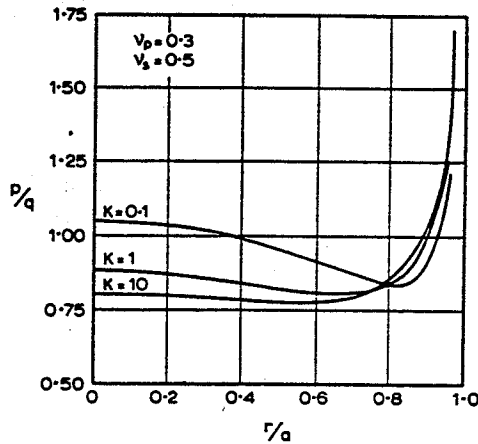


FIG.12.34 Contact pressure distributions. $h/a=1$.
(Brown, 1969a).

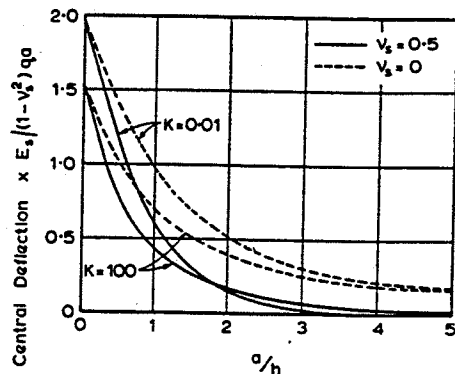


FIG.12.35 Central deflection. $v_p=0.3$. (Brown, 1969a).

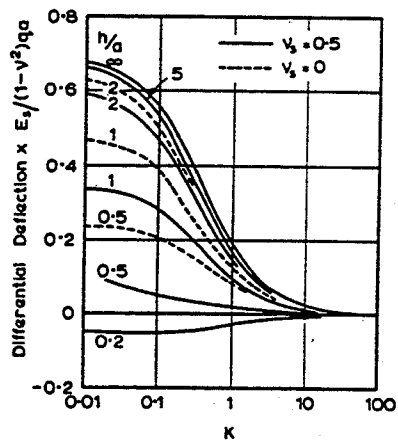


FIG.12.36 Differential deflections. $v_p=0.3$.
(Brown, 1969a).

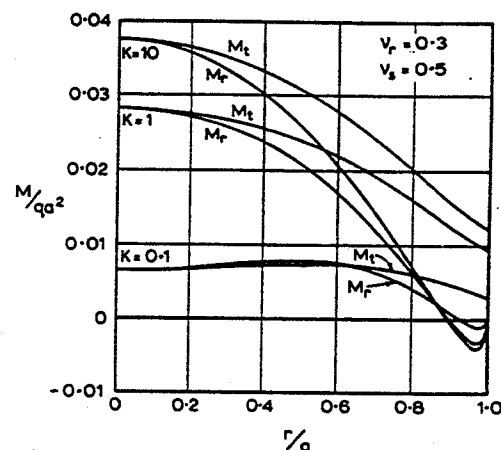


FIG.12.37 Bending moment distributions. $h/a=1$.
(Brown, 1969a).

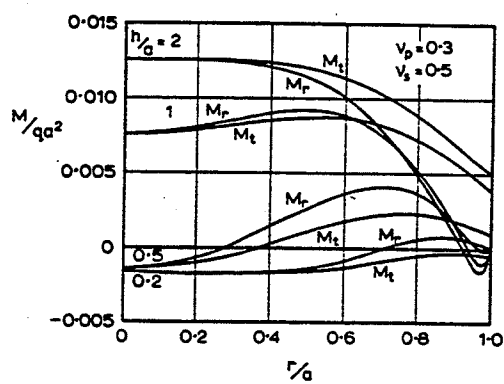


FIG.12.38 Bending moment distributions. $K=0.1$.
(Brown, 1969a).

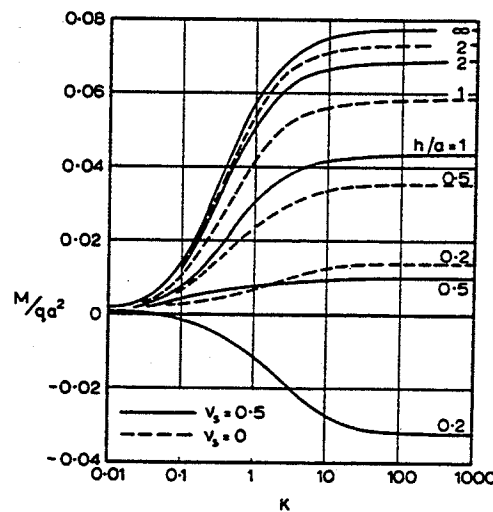


FIG.12.39 Variation of maximum moment with K .
 $v_p=0.3$. (Brown, 1969a).

where E_s, v_s = soil moduli
 D = flexural rigidity of slab.

The displacement and rotation of a rigid rectangular raft are considered in Section 7.6.

Distributions of contact pressure for two rectangles are shown in Fig.12.41 (Butterfield and Banerjee, 1971).

Brown (1972) has obtained solutions for reaction, shear force, bending moment and torsional moment in rigid rectangular rafts. The raft proportions and the loading cases considered are shown in Fig.12.42. Contours representing the solutions are shown in Figs. 12.43 to 12.51. The shear force and moments are expressed in terms of the values per unit width of raft. In all cases, Poisson's ratio of the raft, v_r , is 0.15. In Brown's notation, the shear forces in the x and y directions are denoted as Q_x and Q_y , the bending moments as M_x and M_y , and the torsional moment as M_{xy} . The solutions have been obtained by numerical integration of the biharmonic equation.

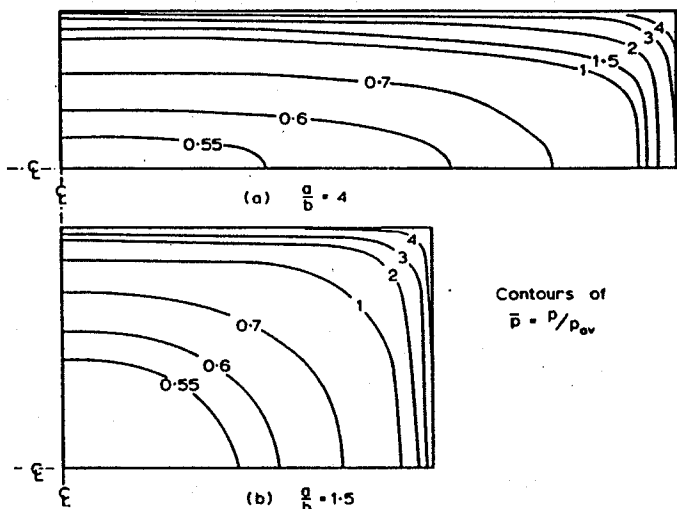


FIG.12.41 Contact pressure distribution beneath rigid rectangular raft (Butterfield and Banerjee, 1971).

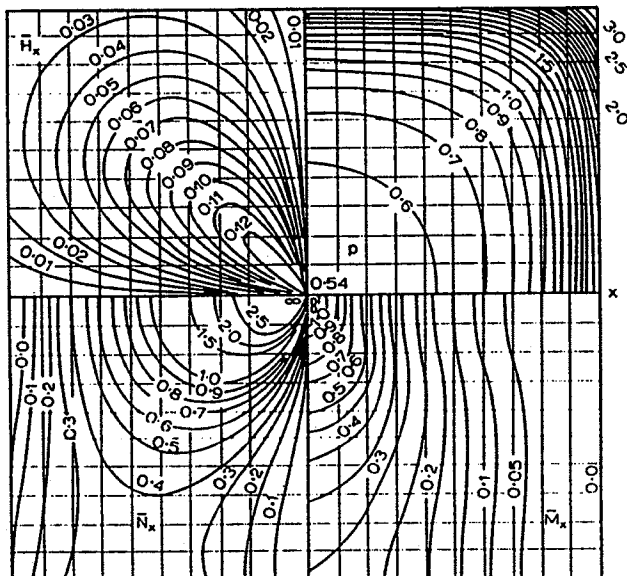


FIG.12.40 Dimensionless reaction, bending moment, torsional moment and shear force in rigid square raft with central concentrated load (Gorbunov-Possadov and Serebrjanyi, 1961).

12.3.2 FLEXIBLE RAFT ON SEMI-INFINITE MASS

Gorbunov-Possadov and Serebrjanyi (1961) have obtained solutions for contact pressure, vertical displacement and moments in a large rectangular raft subjected to concentrated load at the middle of the edge. Influence factors are shown in Fig.12.52.

$$\text{Contact pressure } p = \bar{p} \frac{P}{L^2} \quad \dots (12.21a)$$

$$\text{Vertical displacement } \rho_z = \bar{\rho} \frac{(1-v_s^2) P}{E_s L} \quad \dots (12.21b)$$

$$\text{Moment in } x\text{-direction } M_x = \bar{M}_x P \quad \dots (12.21c)$$

$$\text{Moment in } y\text{-direction } M_y = \bar{M}_y P \quad \dots (12.21d)$$

$$\text{where } L = \left(\frac{2D(1-v_s^2)}{E_s} \right)^{1/3}$$

$$\xi = \frac{x}{L}$$

$$\eta = \frac{y}{L}$$

P, D, E_s, v_s are defined in the previous section.

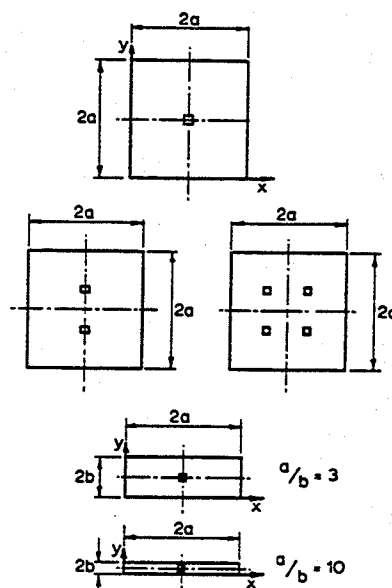


FIG.12.42 Loading cases for rigid rafts (Brown,1972).

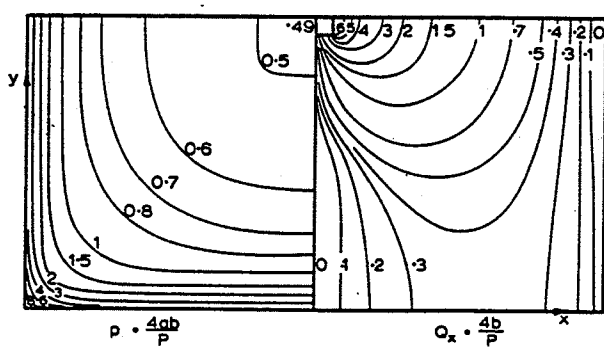


FIG.12.43 Reaction and shear distributions for rigid square raft with central load (Brown, 1972).

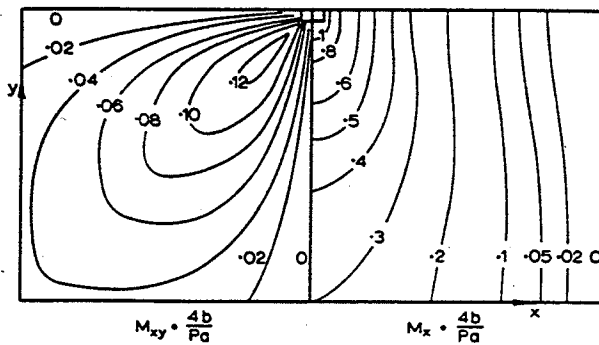


FIG.12.44 Torsional and bending moments for a rigid square raft with central load (Brown, 1972).

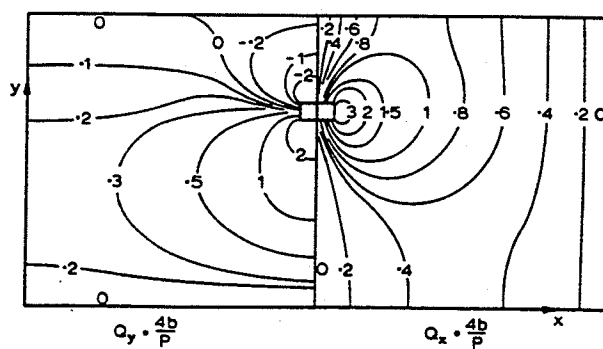


FIG.12.45 Shear force distributions for rigid square raft subjected to two loads (Brown, 1972).

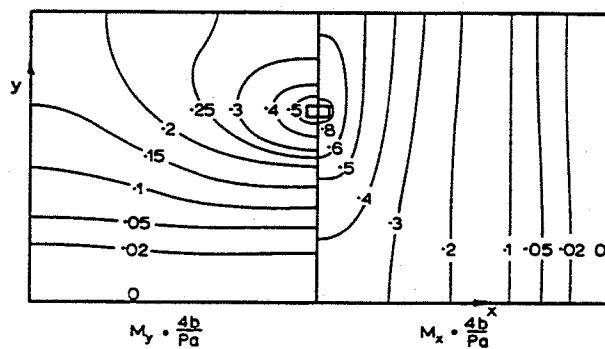


FIG.12.46 Bending moments for rigid square raft subjected to two loads (Brown, 1972).

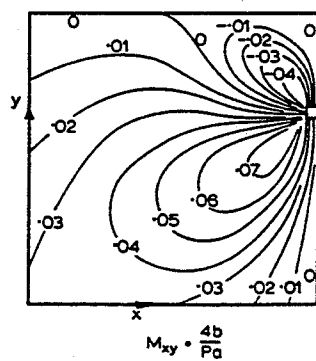


FIG.12.47 Torsional moments for rigid square raft subjected to two loads (Brown, 1972).

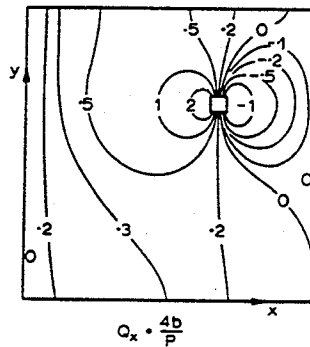


FIG.12.48 Shear force distribution for rigid square raft subjected to four loads
(Brown, 1972).

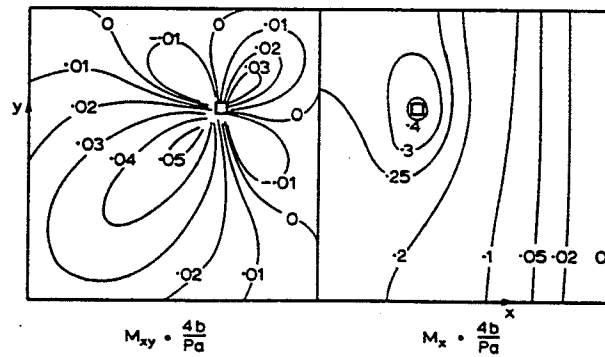


FIG.12.49 Bending and torsional moments for rigid square raft subjected to four loads (Brown, 1972).

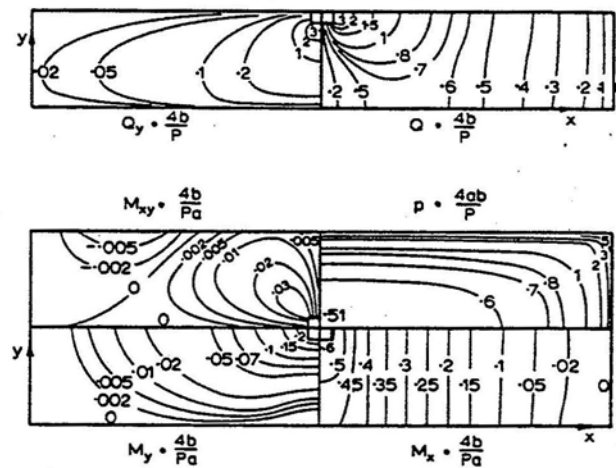


FIG.12.50 Behaviour of rigid raft with central load.
 $a/b=3$ (Brown, 1972).

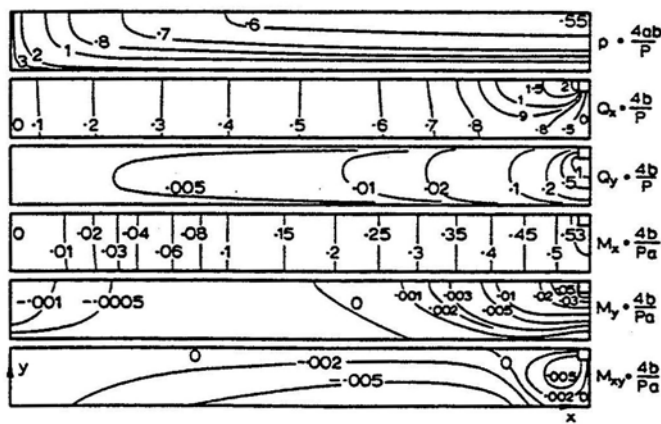


FIG.12.51 Behaviour of rigid raft with central load.
 $a/b=10$ (Brown, 1972).

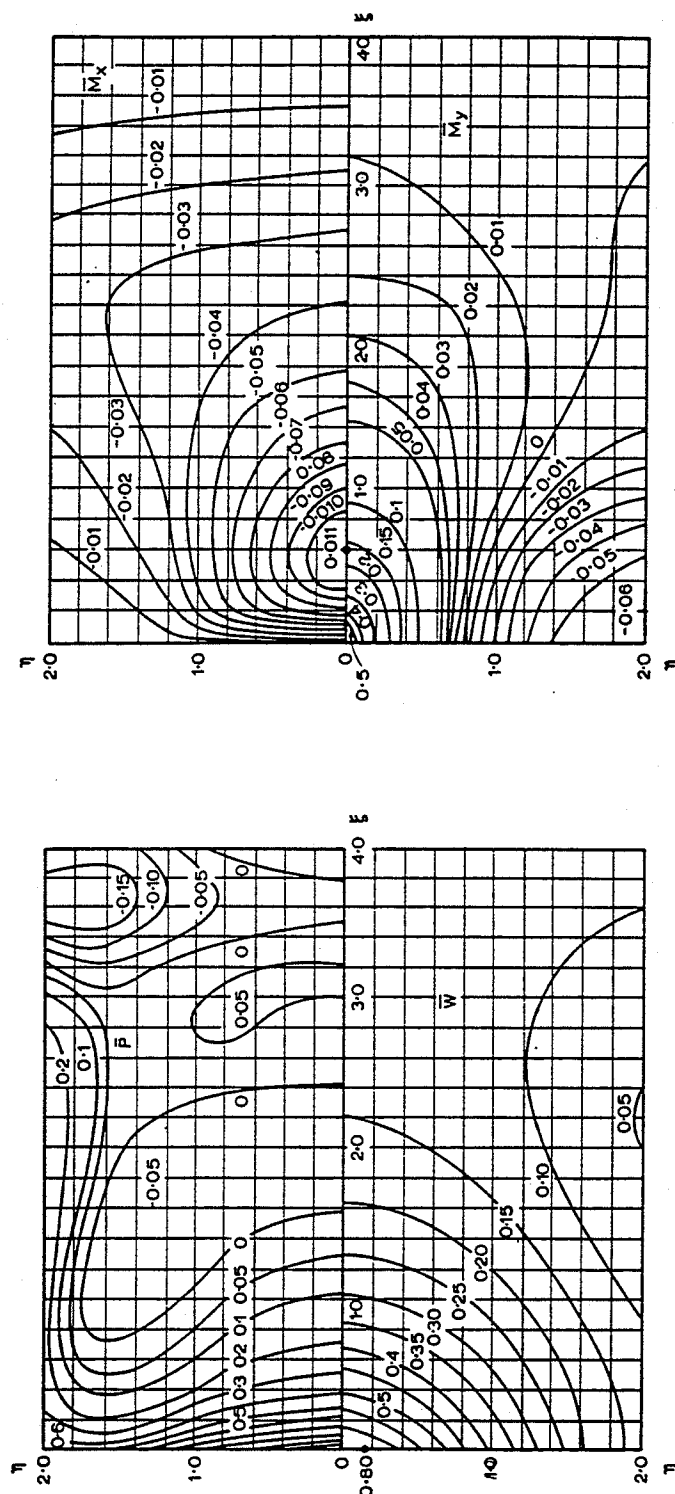


FIG.12.52 Dimensionless reaction, bending moments and vertical displacement for square raft subjected to concentrated load at edge (Gorbunov-Possadov and Serebryanyi, 1961).